Journal of Quantitative Spectroscopy & Radiative Transfer 146 (2014) 175–180

Contents lists available at ScienceDirect

Journal of Quantitative Spectroscopy & Radiative Transfer

journal homepage: www.elsevier.com/locate/jqsrt

On the understanding of local optical resonance in elongated dielectric particles

J. Bogdanowicz [a,b,*], W. Vandervorst [a,b]

[a] Instituut voor Kern- en Stralingsfysika, KU Leuven, Celestijnenlaan 200D, B-3001 Leuven, Belgium
[b] IMEC, Kapeldreef 75, B-3000 Leuven, Belgium

ARTICLE INFO

Article history:
Received 7 October 2013
Received in revised form
20 January 2014
Accepted 22 January 2014
Available online 30 January 2014

Keywords:
Mie resonance
Atomprobe tomography
Absorption
Silicon

ABSTRACT

This paper discusses the peculiar light coupling and absorption properties of a dielectric particle with a varying nanoscale radius and a high aspect ratio. To build progressive understanding, different levels of geometrical refinement with increasing complexity are proposed and compared. This study concludes that, in an elongated dielectric particle with a varying radius, light is coupled and absorbed only at optically resonant positions, i.e. where the radius allows for the constructive interference between the multiple internal reflections occurring inside the particle. The position, extension and magnitude of these resonance maxima, which vary according to the refinement level of the model, are discussed.

1. Introduction

The problem of the interaction of light with elongated dielectric particles is of high relevance to many fields of investigation [1–4]. Recently, since the advent of the laser-assisted Atom Probe Tomography (APT) technique and its demonstrated ability to measure and reconstruct nanostructures such as FinFETs or nanowires in three dimensions [5], the specific question of the light coupling and absorption in nanoscale semiconducting cones has been pushed to the forefront. In this context, it has been shown that light couples into elongated tips such as that used in APT only at specific, optically resonant, locations of the tip [6,7]. This enhancement of the internal electromagnetic field has been attributed to local Mie resonance [6,8]. However, deep insight into the physics and dependencies of this resonance phenomenon is still missing. The present paper aims at uncovering the physical grounds of the local optical resonance and, hence, understanding the main mechanisms and parameters which determine the electromagnetic field distribution inside an illuminated elongated tip.

This paper is structured as follows. We propose to build progressive understanding by addressing first the interaction between light and particles with a simplified *two-dimensional* geometry, i.e. particles with an infinite thickness. We then investigate the impact of the finite thickness of a *three-dimensional* elongated object. The different geometries considered are schematically illustrated in Fig. 1, which also specifies the case study of this paper, i.e. a conical silicon tip with a cone angle $\alpha = 2^{\circ}$, an apex radius $R_{apex} = 25$ nm, a 3 μm length and a complex refractive index $\tilde{n} = n + ik = 4.22 + 0.039i$ [9] illuminated by a plane wave with amplitude E_0 and wavelength $\lambda_0 = 515$ nm polarized along the z axis of the particle and incident normally to this axis. In the sequel, we omit the factor $\exp(-i\omega t)$ expressing the time dependence of the waves involved in this paper, ω being the angular frequency of the incident light.

2. Two-dimensional geometries

Neglecting the impact of the finite thickness of a three-dimensional particle is, in the optical interaction problem of this paper like in any other physical problem, a most simplifying approximation. First and foremost, assuming

* Corresponding author.
E-mail address: janusz.bogdanowicz@imec.be (J. Bogdanowicz).

0022-4073/$ - see front matter © 2014 Elsevier Ltd. All rights reserved.
http://dx.doi.org/10.1016/j.jqsrt.2014.01.016

that the aspect ratio of the particle is large enough, geometrical optics can be used to predict the propagation of the optical waves inside the particle, which drastically reduces the complexity of this problem. This approximation is widely used in the context of scattering and interference in thin-film and wedge geometries [10,11] and has been experimentally proven to be accurate at a scale smaller than the wavelength, i.e. down to nanometer thicknesses [12–14]. Second, it enables one to focus on a plane geometry, which strongly facilitates the visualization. Besides, as we shall see, most of the qualitative physics of the interaction remains valid in spite of the simplified geometry. We propose below to first consider the case of an illuminated stack of thin films and to proceed with the study of a truncated wedge (Fig. 1).

2.1. Stack of thin films

Approximating an elongated three-dimensional particle by a stack of thin films is quite a crude simplification. This indeed leads to neglecting the impact not only of the thickness of the particle but also of its tilted walls with respect to the propagation direction of the incident light (Fig. 1). However, the analytical solution to this problem offers very easily accessible qualitative understanding, which justifies its presence in this paper.

When light impinges normally on a dielectric slab of half-thickness $R(z)$, it is transmitted and then bounces back and forth internally, leading to constructive or destructive interference according to the ratio $\lambda_0/[nR(z)]$. Let us go through the various waves generated inside the slab and involved in the interference. First, when the incident wave

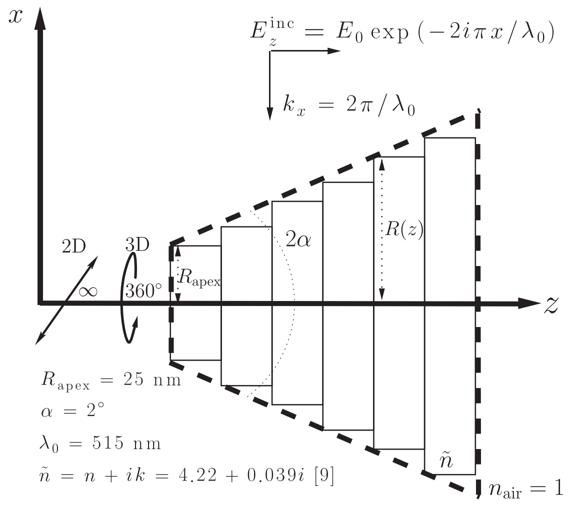

Fig. 1. Geometries of the different approximations of a conical dielectric particle with cone angle $\alpha=2°$, apex radius $R_{\mathrm{apex}} = 25$ nm and complex refractive index $\tilde{n} = 4.22+0.039i$ [9] illuminated by a plane wave with wavelength $\lambda_0=515$ nm polarized along the z axis of the particle and incident normally to this axis. The two-dimensional (2D) approximations, i.e. the stack of thin films (full lines) and the truncated wedge (interrupted lines), are obtained assuming an infinite thickness in the direction perpendicular to the figure. The three-dimensional (3D) geometries, i.e. the stack of cylinders (full lines) and the truncated cone (interrupted lines), are obtained by applying a 360° rotation of the particle around the z axis.

of amplitude E_0 crosses the air–Si interface, it generates the so-called *transmitted wave*, i.e. a downward-propagating wave of amplitude $\tilde{t}_0^{\perp} E_0$, where $\tilde{t}_0^{\perp} = 2/(\tilde{n}+1)$ is the normal-incidence air-to-Si transmission coefficient [11]. We consider the air–Si interface as the origin of the phase, i.e. the point at which the transmitted wave has a null phase. Next, when the transmitted wave reaches the bottom Si–air interface, the upward-propagating *first reflected wave* is generated with an amplitude $\tilde{r}^{\perp}\tilde{t}_0^{\perp} E_0$, $\tilde{r}^{\perp} = (\tilde{n}-1)/(\tilde{n}+1)$ being the normal-incidence internal reflection coefficient [11]. The *second reflected wave*, i.e. a downward wave with amplitude $(\tilde{r}^{\perp})^2\tilde{t}_0^{\perp} E_0$, is then generated when the first reflected wave reaches the top Si–air interface. An infinite number of reflected waves have to be considered, though the transmission loss reduces their amplitude by a factor $\tilde{r}^{\perp}$ at each internal reflection. The total internal electric field $E_{z,\,\mathrm{int}}$ at position x inside one of the slabs of Fig. 1 can therefore be written as the coherent sum of the transmitted wave and all the subsequent reflected waves, i.e.

$$\begin{aligned} E_{z,\,\mathrm{int}}(x) = E_0\tilde{t}_0^{\perp} \Bigg\{ & \underbrace{\exp[-2i\pi\tilde{n}(x-R(z))/\lambda_0]}_{\text{transmitted wave}} \\ & + \underbrace{\tilde{r}^{\perp}\exp[2i\pi\tilde{n}(x+3R(z))/\lambda_0]}_{1^{\text{st}}\text{ reflected wave}} \\ & + \underbrace{(r^{\perp})^2\exp[-2i\pi\tilde{n}(x-R(z))/\lambda_0]\exp[8i\pi\tilde{n}R(z)/\lambda_0]}_{2^{\text{nd}}\text{ reflected wave}} \\ & + \underbrace{(\tilde{r}^{\perp})^3\exp[2i\pi\tilde{n}(x+3R(z))/\lambda_0]\exp[8i\pi\tilde{n}R(z)/\lambda_0]}_{3^{\text{rd}}\text{ reflected wave}} + \ldots \Bigg\} \end{aligned} \quad (1)$$

$$\begin{aligned} = E_0\tilde{t}_0^{\perp}\{ & \exp[-2i\pi\tilde{n}(x-R(z))/\lambda_0] \\ & + \tilde{r}^{\perp}\exp[2i\pi\tilde{n}(x+3R(z))/\lambda_0]\}\frac{1}{1-(r^{\perp})^2\exp[8i\pi\tilde{n}R(z)/\lambda_0]}. \end{aligned} \quad (2)$$

Note that, using the electromagnetic theory of light, i.e. by application of the boundary conditions of Maxwell's equations, an expression identical to Eq. (2) can be found [10].

Fig. 2(a) shows the squared relative amplitude $|E_{z,\,\mathrm{int}}/E_0|^2$ of the resulting internal field obtained when generalizing the use of Eq. (2) to the case of the stack of thin films with varying half-thickness $R(z)$ of Fig. 1. As a result of the constructive and destructive interference between the numerous waves propagating perpendicularly to the axis of the particle, the internal field shows a periodic pattern of maxima and minima, the maxima being located along the z axis in the regions where $R(z)$ is a multiple of $\lambda_0/(4n)$, as is typical for thin-film interference. The positions of resonance are strictly only linked to the local thickness and independent from the particle shape and therefore from the apex radius or the angle α. Though the overall pattern is due to the interference between an infinite number of waves, it can easily be shown that the first six terms of Eq. (1), which we call the *primary waves*, account for most of the observed interference pattern. The waves undergoing further internal